Jana et al., J Material Sci Eng 2015, 4:4
DOI: 10.4172/2169-0022.1000181

Journal of Material Sciences & Engineering

Research Article Open Access

Influence of Biofield Treatment on Physical, Structural and Spectral Properties of Boron Nitride

Trivedi MK[1], Patil S[1], Nayak G[1], Jana S[2]* and Latiyal O[2]

[1]*Trivedi Global Inc., 10624 S Eastern Avenue Suite A-969, Henderson, NV 89052, USA*
[2]*Science Research Laboratory Pvt. Ltd., Hall-A, Chinar Mega Mall, Chinar Fortune City, Hoshangabad Rd., Bhopal-462026 Madhya Pradesh, India*

Abstract

Boron nitride (BN) is known for high hardness, thermal stability, thermal conductivity, and catalytic action. The aim of this study was to investigate the effect of biofield treatment on physical, structural and spectral properties of BN powder. The control and treated sample of BN powder were characterized by X-ray diffraction (XRD), surface area analysis and Fourier transform infrared spectroscopy (FT-IR). XRD results indicated that biofield treatment had substantially changed the crystallinity of BN powder as compared to control. Apart from the crystallinity, significant changes were also observed in lattice parameter, density and molecular weight of the treated BN powder as compared to control sample. The XRD data confirmed 33.30% increase crystallite size in treated BN powder as compared to control. The surface area data showed 10.33% increment in surface area of treated BN as compared to control. Furthermore, FT-IR spectra revealed that some part of BN may be transformed from hexagonal BN (h-BN) to rhombohedral boron nitride (r-BN), which was corroborated by emergence of new prominent peaks at 1388 cm^{-1} in treated BN as compared to control sample. These findings suggest that biofield treatment has substantially altered the structural properties and surface area of treated BN powder.

Keywords: Biofield treatment; Boron nitride; X-ray diffraction; FT-IR; Surface area

Introduction

Boron nitride (BN) is a well-known ceramic material with fascinating properties, such as low density, high melting point, strength, corrosion resistance, and good chemical stability, excellent electrical and thermal properties. These properties make boron nitride a promising material for a wide range of industrial applications, especially for its uses under extreme high temperature conditions [1-3]. The BN originally exists in several crystal structures such as wurtzite BN (w-BN), cubic BN (c-BN), rhombohedral BN (r-BN), hexagonal BN (h-BN), explosive BN (e-BN), and turbostratic BN (t-BN). The c-BN and w-BN are especially known for super-hardness, wide band gap and its oxidation resistance which makes them a promising material for fabrication of cutting tools, protective coatings, and optoelectronic devices [4,5].

Nevertheless, the h-BN has similar crystal structure to graphite hence it is also known as white graphite [6,7]. This crystal structure provides the outstanding lubricating properties, high thermal conductivity, electrical resistance and low dielectric constant [4,8,9]. Recently, BN is synthesized with various morphologies, such as hollow spheres [10], porous structures [11], and one-dimensional nanostructures to obtained excellent properties [12,13]. The porous BN has gain significant attention due to its high specific surface area, which makes it a promising material for catalytic action. The porous BN has been synthesized by using various methods such as molecular precursors, and supercritical drying method etc [14-17]. However, all these methods require either special precursor or high temperature conditions to modulate the specific surface area and crystal structure. In physics, the energy is considered as the ability to do work; which fundamentally interrelates with matter as $E=mc^2$ (Einstein's famous equation). However the energy can be considered as a field of force which effectively interacts with any matter at a distance and cause action.

Researchers have confirmed that biomagnetic fields are present around human body, which have been evidenced by electromyography (EMG), electrocardiography (ECG) and electroencephalogram (EEG) [18]. Scientists have postulated that it is due to the flow of bioelectricity (generated from heart, brain functions or due to the motion of charged particles such as protons, electrons, and ions) in the human body. As per the basic fundamental law in physics, when an electrical signal passes through any material, a magnetic field is generated in the surrounding space. Hence, a magnetic field is created along with the bioelectricity in human body, known as biomagnetic field. The cumulative field created by bioelectricity and biomagnetic field, which surrounding the human body is known as biofield. The energy associated with this field is considered as biofield energy.

Mr. Mahendra K Trivedi's biofield has known to alter the characteristics in various things at atomic, molecular and physical level in many fields such as material science [19-26], microbiology [27-29], biotechnology [30,31] and agriculture [32-34]. The biofield treatment has also shown significant results in graphite carbon, for instance, the unit cell volume was decrease by 1% and crystallite size was increased by 100% after treatment [20]. In the present study, we report for the first time, an impact of biofield treatment on BN powder for its structural properties along with atomic and physical properties.

Experimental

The BN powder was purchased from Sigma Aldrich, USA. The sample was equally divided into two parts, one part was considered as control and other part was exposed to Mr. Trivedi's biofield, herein

***Corresponding author:** Snehasis Jana, Trivedi Science Research Laboratory Pvt. Ltd., Hall-A, Chinar Mega Mall, Chinar Fortune City, Hoshangabad Rd., Bhopal- 462026, Madhya Pradesh, India, Tel: +91-755-6660006; E-mail: publication@trivedisrl.com

Received June 18, 2015; **Accepted** July 13, 2015; **Published** July 23, 2015

Citation: Trivedi MK, Patil S, Nayak G, Jana S, Latiyal O (2015) Influence of Biofield Treatment on Physical, Structural and Spectral Properties of Boron Nitride. J Material Sci Eng 4: 181. doi:10.4172/2169-0022.1000181

referred as biofield treatment. The control and treated samples were characterized using X-ray Diffraction (XRD), surface area analyzer, and Fourier transform infrared (FT-IR) spectroscopy.

X-ray diffraction study

For X-ray diffraction study the treated sample was divided into four parts, coded as T1, T2, T3, and T4 respectively. The XRD analysis was performed on X-ray diffractometer Phillips, Holland PW 1710 system with a copper anode with nickel filter and wavelength of radiation of 1.54056 Å. The data provided by XRD system was in the form of a chart of 2θ vs. intensity and a table containing peak intensity counts, d value (Å), peak width (θ°), and relative intensity (%) etc. For computing lattice parameter and unit cell volume, PowderX software was used.

Crystallite size (G) was calculated using following equation:

$$G=k\lambda/(b\cos\theta),$$

Where k is the equipment constant (0.94) and λ is the wavelength of radiation (1.54056 Å). The molecular weight of a molecule is the sum of the atomic weight of all atoms and the atomic weight is the sum of the total weight of protons, neutrons and electrons present in an atom. Since the number of molecules in a unit cell is fixed so the weight of the unit cell was computed as, number of molecules present in a unit cell multiplied by the molecular weight. The density was calculated as weight of the unit cell divided by volume of the unit cell. The percent change in lattice parameter "a" was calculated by using following equation:

$$\text{Percent change in lattice parameter}=[(a_t-a_c)/a_c] \times 100$$

Where a_c and a_t are lattice parameter of control and treated powder samples respectively. The percentage change in all other parameters such as unit cell volume, density, and crystallite size was calculated in a similar manner.

Surface area analysis

The surface area was characterized using surface area analyzer, SMART SORB 90 BET, which had a detection range of 0.1–1000 m^2/g.

Infrared spectroscopy

FT-IR analysis of control and treated samples T1, T2 was carried out on Shimadzu, Fourier transform infrared (FT-IR) spectrometer with frequency range of 300–4000/cm.

Results and Discussion

X-ray diffraction (XRD)

The XRD patterns of control and treated BN powder are shown in Figures 1a-1e. The XRD diffractogram of control BN samples showed diffraction peaks at 2θ=26.81°, 41.59°, 50.10°, and 55.13°. The XRD of treated BN sample showed peaks as, T1: 2θ=26.75°, 41.60°, 50.16°, 55.11°; T2: 2θ=26.73°, 41.57°, 50.10°, 55.11°; T3: 2θ=26.70°, 41.51°, 55.06°, 55.05°; T4: 2θ=26.74°, 41.57°, 50.14°, 55.11°. These four peaks in control and treated samples were attributed to the crystalline planes (002), (100), (102) and (004), which were in agreement with Joint Committee on Powder Diffraction Standards (JCPDS) card no. 34-0421 [35]. These peaks confirmed the hexagonal crystal structure of BN (h-BN) in all the control and treated samples. The intensity of diffraction peaks along plane (002) was reduced in treated BN sample (T2 and T4), which indicated that crystallinity was decreased after biofield treatment (Figures 1c and 1e). The XRD data was analyzed using PowderX software to calculate lattice parameter, unit cell volume, density,

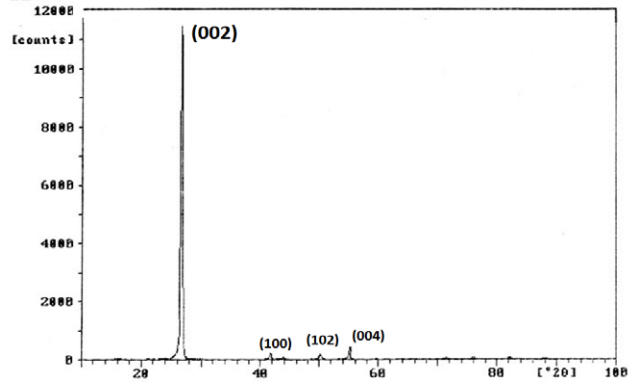

Figure 1a: XRD pattern of control BN sample.

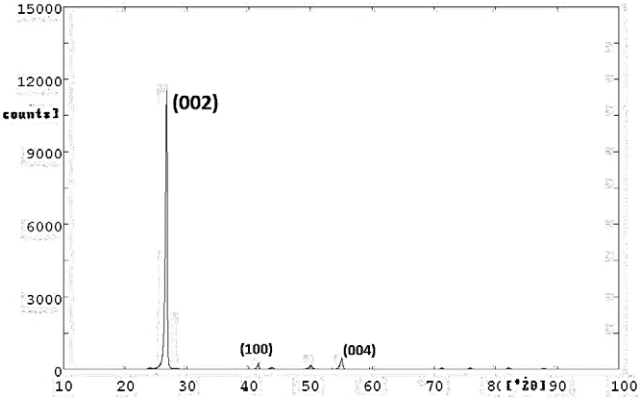

Figure 1b: XRD pattern of biofield treated BN sample T1.

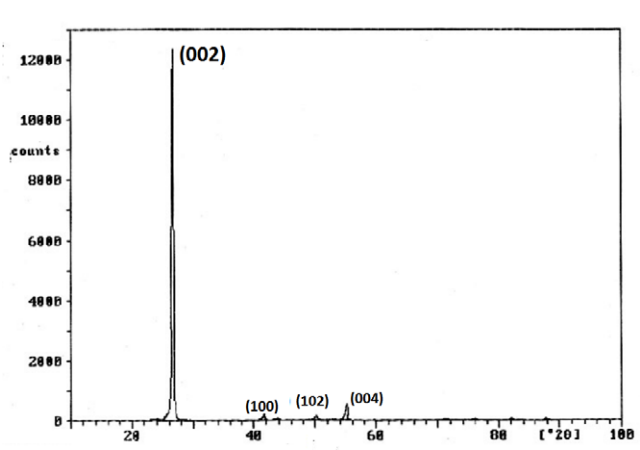

Figure 1c: XRD pattern of biofield treated BN sample T2.

molecular weight and crystallite size, which are presented in Table 1. It was found that the lattice parameter of the unit cell was increased in treated sample T2 by 0.16% after treatment (Figure 2) as compared to control. A positive lattice strain in treated BN samples indicated that a tensile stress may be applied over the unit cell [24]. This may led to increase the unit cell volume by 0.33% and reduced density by 0.33% in treated BN samples as compared to control.

Furthermore, when tensile stress was applied on the atoms of

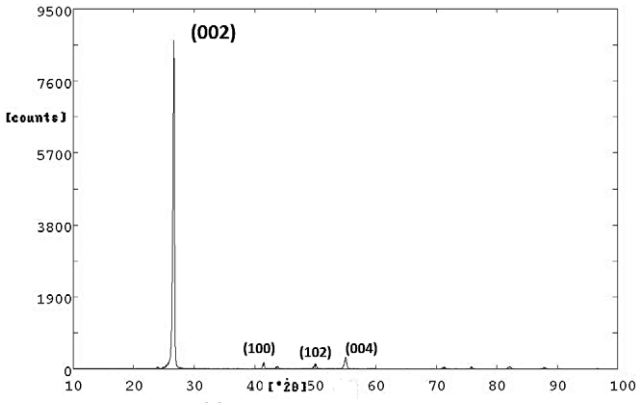

Figure 1d: XRD pattern of biofield treated BN sample T3.

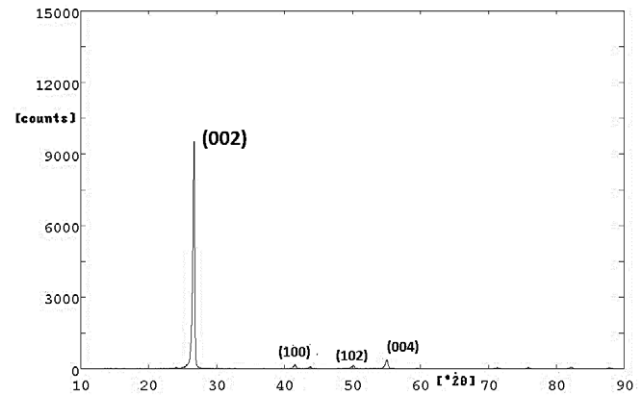

Figure 1e: XRD pattern of biofield treated BN sample T4.

	Lattice Parameter (Å)	Unit cell volume (× 10^{-23} cm^3)	Density (g/cc)	Molecular Weight (g/mol)	Crystallite Size (nm)
Control sample	2.5040	3.6121	2.318	25.21	35.44
Treated T1	2.5046	3.6137	2.317	25.23	38.65
Treated T2	2.5064	3.6191	2.313	25.26	35.43
Treated T3	2.5081	3.6240	2.310	25.30	47.24
Treated T4	2.5054	3.6160	2.315	25.24	47.24

Table 1: X-ray diffraction (XRD) of lattice parameter, unit cell volume, density, molecular weight and crystallite size of BN sample.

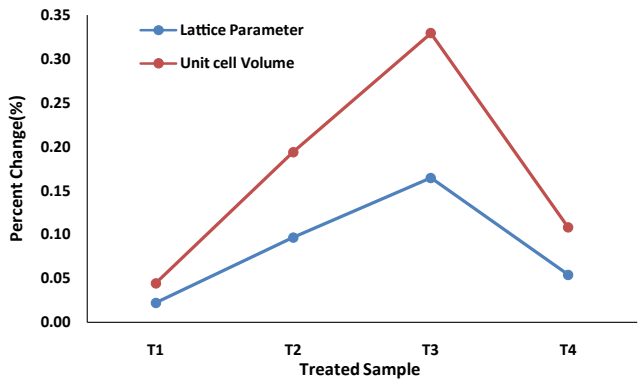

Figure 2: Percentage change in lattice parameter and volume of unit cell of treated BN as compared to control.

BN, the electron cloud, around the nucleus moved away from the centre that may led to increased atomic size [19]. Consequently, the increased atomic size may reduce the nuclear charge per unit volume. Furthermore, it was observed that the molecular weight in treated BN samples were increased up to 0.33% as compared to control (Figure 3). The reduction in nuclear charge per unit volume and increased molecular weight suggested that the number of protons were probably decreased in treated BN powder. It can be possible only when protons are participating in reversible weak nuclear reactions giving rise to neutrinos and neutrons [21-23,36]. Additionally, it was found that the crystallite size was increased up to 33.30% in treated BN sample as compared to control (Figure 4). It is possible that the internal strains present in treated BN powder made dislocations to move unhindered that results into reorient the planes on either side of the crystallite boundaries. Further, this reorientation of planes may led to increase the crystallite size [25]. Al-Jawhari reported that the crystallite size have direct relationship with dielectric constant [17]. Moreover, the dependence of dielectric constant on the crystallite size has been reported by researchers on other materials such as diamond, TiO_2 and Bi_2O_3, where it was mentioned that dielectric constant increases as crystallite size increases [37-39]. Thus, it is hypothesized that the biofield treatment may enhance the dielectric constant of BN powder.

Surface area analysis

The surface area analysis of control and treated BN powder is presented in Figure 5 and Table 2. It was found that the specific surface area was increased by 10.22%, 4.25% and 10.33% in treated BN samples T1, T2 and T3, respectively as compared to control. This was probably due to the reduction in particle size through high internal strain and energy milling provided by biofield treatment. Furthermore, it is postulated that high energy milling may produce the porosity over

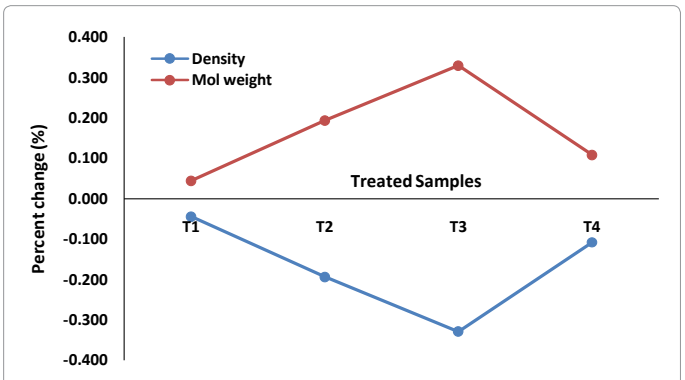

Figure 3: Percentage change in lattice parameter and volume of unit cell in biofield treated BN as compared to control.

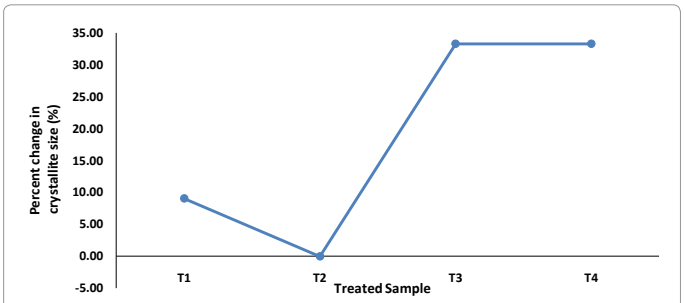

Figure 4: Percentage change in crystallite size of biofield treated BN powder as compared to control.

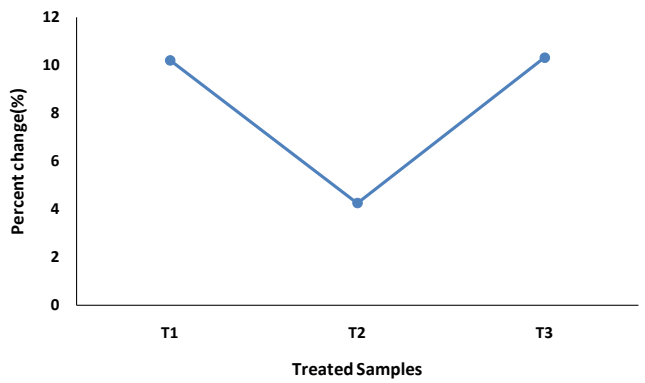

Figure 5: Percentage change in surface area of biofield treated BN powder as compared to control.

	Surface Area (m^2/g)	% change in Surface Area
Control	3.68	-
Treated T1	4.06	10.22
Treated T2	3.84	4.25
Treated T3	4.06	10.33

Table 2: Surface area of control and treated BN samples.

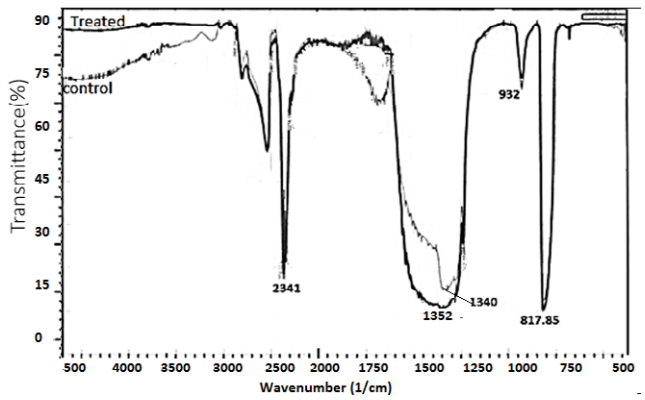

Figure 6: FT-IR spectrum of control and biofield treated BN powder sample (T1).

the particle surface through surface grinding and internal friction. Hence, this higher porosity may result in large surface area in treated BN powder as compared to control [15,16]. Moreover, this increased surface area would be helpful to confer better performance during catalytic applications.

FT-IR spectroscopy

Figures 6 and 7 shows the FT-IR spectra of control and treated BN powder. The absorption peaks near 1340 cm^{-1} was attributed to E_{1u} in plane sp^2 bonded B-N stretching vibrations and the peak at 817 cm^{-1} was corresponded to A_{1u} out of plane B-N-B bonding vibrations in the control BN powder [35]. The treated sample T1 (Figure 6) showed absorption peaks at around 923/cm which was attributed to the presence of e-BN along with h-BN in control and treated (T1 and T2) powder (Figures 6 and 7). One interesting absorption peak was observed in IR spectrum of treated sample (T2) at 1124/cm (Figure 7) which was mainly due to presence of w-BN, however this peak was absent in control sample [40]. It revealed that some amount of h-BN may be transformed into w-BN due to biofield treatment. The FT-IR

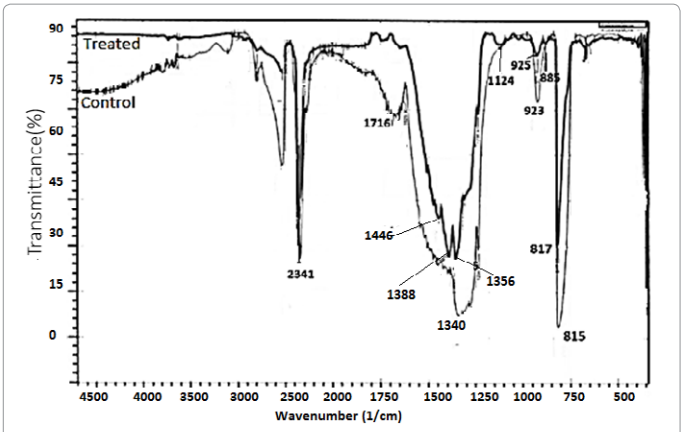

Figure 7: FT-IR spectrum of control and biofield treated BN powder sample (T2).

spectrum of control sample showed an absorption peak at around 1340/cm and interestingly two peaks were found at 1388/cm and 1356/cm in treated sample (T2). The emergence of new absorption peak at 1388/cm could be due to the presence of r-BN [35]. It is postulated that the h-BN unit cell was distorted to form r-BN unit cell, which may be due to applied tensile stress during high energy milling through biofield treatment. Based on these results, it is assumed that, biofield treatment could be an alternative technique to modulate the physical and atomic characteristic in BN powder for optoelectronic and chemical industries.

Conclusion

Present study, concludes that the biofield treatment has significantly changed the atomic and crystal structural characteristics of BN powder. XRD data confirmed that the crystallite size was significantly increased up to 33.3% in treated BN powder as compared to control, which may directly increase the dielectric constant. Furthermore, the FT-IR results revealed that h-BN crystal structure may be transformed into r-BN after biofield treatment. The higher surface area in treated BN was found as compared to control, indicating that it could be more useful during the catalytic reaction. Based on these promising results, it is expected that biofield treatment could be applied to improve the catalytic and optoelectronic properties of BN powder.

Acknowledgement

Authors gratefully acknowledged to Dr. Cheng Dong of NLSC, Institute of Physics, and Chinese academy of Sciences for providing the facilities to use PowderX software for analyzing XRD data.

References

1. Paine RT, Narula CK (1990) Synthetic routes to boron nitride. Chem Rev 90: 73-91.
2. Watanabe K, Taniguchi T, Kanda H (2004) Direct-bandgap properties and evidence for ultraviolet lasing of hexagonal boron nitride single crystal. Nature Mater 3: 404-409.
3. Mirkarimi PB, McCarty KF, Medlin DL (1997) Review of advances in cubic boron nitride film synthesis. Mater Sci Eng Rep 21: 47-100.
4. Shi X, Wang S, Yang H, Duan X, Dong X (2008) Fabrication and characterization of hexagonal boron nitride nanopowder by spray drying and calcining-nitriding technology. J Solid State Chem 181: 2274-2278.
5. Lian G, Zhang X, Zhu L, Tan M, Cui D, et al. (2010) New strategies for selectively synthesizing cubic boron nitride in hydrothermal. Cryst Eng Comm 12: 1159-1163.
6. Bindal MM, Singh BP, Singhal SK, Nayar RK, Chopra R (1994) High pressure

phase transformations in turbostratic boron nitride using magnesium boron nitride as the catalyst. Cryst Growth 144: 97-102.

7. Gladkaya IS, Kremkova GN, Slesarev VN (1986) Turbostratic boron nitride (BNt) under high pressures and temperatures. J Less Common Met 117: 241-245.

8. Laurence Vel L, Demazeau G, Etourneau J (1991) Cubic boron nitride: synthesis, physicochemical properties and applications. Mater Sci Eng B 10: 149-164.

9. Soma T, Sawaoka A, Saito S (1974) Characterization of wurtzite type boron nitride synthesized by shock compression. Mater Res Bull 9: 755-762.

10. Chen LY, Gu YL, Shi L, Yang ZH, Ma JH, et al. (2004) A room-temperature approach to boron nitride hollow spheres. Solid State Comm 130: 537-540.

11. Dibandjo P, Chassagneux F, Bois L, Sigala C, Miele P (2006) Synthesis of boron nitride with a cubic mesostructure. Micropor Mesopor Mater 92: 286-291.

12. Mickelson W, Aloni S, Han WQ, Cumings J, Zettl A (2003) Packing C_{60} in boron nitride nanotubes. Science 300: 467-469.

13. Deepak FL, Vinod CP, Mukhopadhyay K, Govindaraj A, Rao CNR (2002) Boron nitride nanotubes and nanowires. Chem Phys Lett 353: 345-352.

14. Lindquist DA, Smith DM, Datye AK, Johnston GP, Borek TT, et al. (1990) Boron nitride and composite aerogels from borazine-based polymers. Mater Res Soc Symp Proc 180: 1029-1034.

15. Dibandjo P, Bois L, Chassagneux F, Cornu D, Letoffe JM, et al. (2005) Synthesis of boron nitride with ordered mesostructure. Adv Mater 17: 571-574.

16. Borovinskaya IP, Bunin VA, Merzhanov AG (1997) Self-propagating high-temperature synthesis of highly porous boron nitride. Mendeleev Comm 7: 47-48.

17. Perdigon-Melon JA, Auroux A, Guimon C, Bonnetot B (2004) Micrometric BN nanopowders used as catalyst support: Influence of the precursor on the properties of the BN ceramic. J Solid State Chem 177: 609-615.

18. Zahra M, Farsi M (2009) Biofield therapies: Biophysical basis and biological regulations. Complement Ther Clin Pract 15: 35-37.

19. Trivedi MK, Tallapragada RM (2008) A transcendental to changing metal powder characteristics. Met Powder Rep 63: 22-28, 31.

20. Trivedi MK, Tallapragada RM (2009) Effect of superconsciousness external energy on atomic, crystalline and powder characteristics of carbon allotrope powders. Mater Res Innov 13: 473-480.

21. Dhabade VV, Tallapragada RM, Trivedi MK (2009) Effect of external energy on atomic, crystalline and powder characteristics of antimony and bismuth powders. Bull Mater Sci 32: 471-479.

22. Trivedi MK, Patil S, Tallapragada RM (2012) Thought intervention through bio field changing metal powder characteristics experiments on powder characteristics at a PM plant. Future Control and Automation 173: 247-252.

23. Trivedi MK, Patil S, Tallapragada RM (2013) Effect of biofield treatment on the physical and thermal characteristics of silicon, tin and lead powders. J Material Sci Eng 2: 1-7.

24. Trivedi MK, Patil S, Tallapragada RM (2013) Effect of biofield treatment on the physical and thermal characteristics of vanadium pentoxide powder. J Material Sci Eng S11: 001.

25. Trivedi MK, Patil S, Tallapragada RM (2014) Atomic, crystalline and powder characteristics of treated zirconia and silica powders. J Material Sci Eng 3: 144.

26. Trivedi MK, Patil S, Tallapragada RM (2015) Effect of biofield treatment on the physical and thermal characteristics of aluminium powders. Ind Eng Manage 4: 151.

27. Trivedi MK, Patil S, Bhardwaj Y (2008) Impact of an external energy on *Staphylococcus epidermis* [ATCC -13518] in relation to antibiotic susceptibility and biochemical reactions - An experimental study. J Accord Integr Med 4: 230-235.

28. Trivedi MK, Patil S (2008) Impact of an external energy on *Yersinia enterocolitica* [ATCC -23715] in relation to antibiotic susceptibility and biochemical reactions: An experimental study. Internet J Alternat Med 6.

29. Trivedi MK, Patil S, Bhardwaj Y (2009) Impact of an external energy on *Enterococcus faecalis* [ATCC-51299] in relation to antibiotic susceptibility and biochemical reactions-An experimental study. J Accord Integr Med 5: 119-130.

30. Patil S, Nayak GB, Barve SS, Tembe RP, Khan RR (2012) Impact of biofield treatment on growth and anatomical characteristics of *Pogostemon cablin* (Benth). Biotechnology 11: 154-162.

31. Altekar N, Nayak G (2015) Effect of biofield treatment on plant growth and adaptation. J Environ Health Sci 1: 1-9.

32. Shinde V, Sances F, Patil S, Spence A (2012) Impact of biofield treatment on growth and yield of lettuce and tomato. Aust J Basic Appl Sci 6: 100-105.

33. Lenssen AW (2013) Biofield and fungicide seed treatment influences on soybean productivity, seed quality and weed community. Agricultural Journal 8: 138-143.

34. Sances F, Flora E, Patil S, Spence A, Shinde V (2013) Impact of biofield treatment on ginseng and organic blueberry yield. AGRIVITA J Agric Sci 35.

35. Aradi E, Naidoo SR, Billing DG, Wamwangi D, Motochi I, et al. (2014) Ion beam modification of the structure and properties of hexagonal boron nitride: An infrared and X-ray diffraction study. Nucl Instr Meth Phys Res B 331: 140-143.

36. Narlikar JV (1993) Introduction to cosmology. Jones and Bartlett Inc., Cambridge University Press.

37. Al-Jawhari HA, Baeraky TA, Afandi YH (2011) The influence of microwave frequencies at high temperatures on structural properties of h-BN. Intl J Eng Technol 11: 63-66.

38. Ye H, Sun CQ, Hing P (2000) Control of grain size and size effect on the dielectric constant of diamond films. Appl Phys 33: L148-L152.

39. Pamu D, Sudheendran K, Krishna M, Raju KCJ, Bhatnagar AK (2007) Microwave dielectric behavior of nanocrystalline titanium dioxide thin films. Vacuum 81: 686-694.

40. Mirkarimi PB, McCarty KF, Medlin DL (1997) Review of advances in cubic boron nitride film synthesis. Mater Sci Eng R 21: 47-100.